Biometals (2017) 30:217–235
DOI 10.1007/s10534-017-9997-x

Genome-wide exploration of metal tolerance protein (*MTP*) genes in common wheat (*Triticum aestivum*): insights into metal homeostasis and biofortification

Recep Vatansever · Ertugrul Filiz · Seckin Eroglu

Received: 19 January 2017 / Accepted: 21 January 2017 / Published online: 1 February 2017

Abstract Metal transport process in plants is a determinant of quality and quantity of the harvest. Although it is among the most important of staple crops, knowledge about genes that encode for membrane-bound metal transporters is scarce in wheat. Metal tolerance proteins (MTPs) are involved in trace metal homeostasis at the sub-cellular level, usually by providing metal efflux out of the cytosol. Here, by using various bioinformatics approaches, genes that encode for MTPs in the hexaploid wheat genome (*Triticum aestivum*, abbreviated as Ta) were identified and characterized. Based on the comparison with known rice MTPs, the wheat genome contained 20 *MTP* sequences; named as TaMTP1–8A, B and D. All TaMTPs contained a cation diffusion facilitator (CDF) family domain and most members harbored a zinc transporter dimerization domain. Based on motif, phylogeny and alignment analysis, A, B and D genomes of TaMTP3–7 sequences demonstrated higher homology compared to TaMTP1, 2 and 8. With reference to their rice orthologs, TaMTP1s and TaMTP8s belonged to Zn-CDFs, TaMTP2s to Fe/Zn-CDFs and TaMTP3–7s to Mn-CDFs. Upstream regions of *TaMTP* genes included diverse cis-regulatory motifs, indicating regulation by developmental stage, tissue type and stresses. A scan of the coding sequences of 20 *TaMTPs* against published miRNAs predicted a total of 14 potential miRNAs, mainly targeting the members of most diverged groups. Expression analysis showed that several *TaMTPs* were temporally and spatially regulated during the developmental time-course. In grains, *MTPs* were preferentially expressed in the aleurone layer, which is known as a reservoir for high concentrations of iron and zinc. The work identified and characterized metal tolerance proteins in common wheat and revealed a potential involvement of MTPs in providing a sink for trace element storage in wheat grains.

Keywords CDF · Micronutrient · Aleurone · Deficiency · Biofortification

Electronic supplementary material The online version of this article (doi:10.1007/s10534-017-9997-x) contains supplementary material, which is available to authorized users.

R. Vatansever
Department of Biology, Faculty of Science and Arts, Marmara University, Goztepe, 34722 Istanbul, Turkey

E. Filiz
Department of Crop and Animal Production, Cilimli Vocational School, Duzce University, Cilimli, 81750 Duzce, Turkey

S. Eroglu (✉)
Department of Genetics and Bioengineering, Faculty of Engineering, Izmir University of Economics, Balcova, 35330 Izmir, Turkey
e-mail: erogluseckin@gmail.com

Introduction

Metals are incorporated into proteins and activate enzymes, which catalyze essential biological reactions. Thus, a deficiency of metals results in serious

negative impacts on plant biomass (Marschner 2012). Contrastingly, metals can cause toxicity when their concentration is in excess within the cytosol, (Thomine and Vert 2013). Therefore, their cellular concentrations must be tightly regulated to achieve optimum growth. In addition, as a parameter of food quality, metal concentrations in edible parts of the plants raise significant attention for human nutrition. In particular, insufficient intake of Fe and Zn from plant-based diets exacerbates deficiencies of those elements in humans, which are considered among the most widespread nutritional disorders in the world (White and Broadley 2009). To combat this, increasing the concentration of Fe and Zn in edible parts of the staple crops, also known as biofortification, has been considered to be one of the most sustainable approaches to the problem (White and Broadley 2009). A major factor determining the partition of nutrients in plant tissues is their relative sink strengths for the respective metal; where sink strength refers to the competitive ability of an organ to attract assimilates (Marcelis 1996). So, to transfer more of a metal to edible parts of the plant, sink strength can either be increased in the edible organs or decreased in the non-edible parts. For example, increasing Fe sink strength in transgenic rice seeds, by overexpressing ferritin, a protein that captures Fe in a nano-cage structure led to an increase in total seed Fe concentration (Qu et al. 2005). In a different study, a decrease of sink strength in the non-edible flag leaf of rice by disrupting proteins which sequestrate Fe into vacuoles resulted in an increase of total seed Fe concentration (Zhang et al. 2012). At the subcellular level, the sink strength of a particular metal in the cell is generated by the exclusion of this metal from the cytoplasm, which often depends on membrane-bound metal transporter proteins (Clemens et al. 2002).

The plant metal tolerance proteins (MTPs) are divalent-cation/H+ antiporters and generally effluxers of metals out of the cytoplasm (Gustin et al. 2011). MTPs usually act as homodimers and contain six transmembrane domains (TMDs) with cytosolic N- and C-terminals (Lu and Fu 2007; Lu et al. 2009; Kolaj-Robin et al. 2015). MTPs mainly transport Mn, Zn and Fe metals but they also have affinities for other divalent cations such as Ni or Cd (Peiter et al. 2007; Cubillas et al. 2013). MTPs are classified based on their metal specificities, as either of the Mn-, Zn- or Fe/Zn- CDF (cation diffusion facilitator family) type (Montanini et al. 2007). MTPs were further phylogenetically grouped and each phylogenetically distinct cluster was named according to the founding *Arabidopsis thaliana* member of the cluster (Gustin et al. 2011). In *A. thaliana* several MTPs have been characterized. *AtMTP1* is ubiquitously expressed in all tissues and transport Zn into the vacuoles (Kobae et al. 2004). AtMTP3 and AtMTP8 are involved in metal tolerance during the Fe-deficiency response, the former transporting Zn and the latter Mn (Arrivault et al. 2006; Eroglu 2015; Eroglu et al. 2016). AtMTP11 confers Mn tolerance to the plants by transporting Mn into endosomal vesicles which are then secreted out of the cytoplasm (Delhaize et al. 2007; Peiter et al. 2007). AtMTP12 has recently been characterized as a Zn transporter and contrary to other MTPs which contain 6 TMDs, it possesses 14 TMDs and acts as a heterodimer with AtMTP5 (Fujiwara et al. 2015). Knowledge on MTPs is lower in species other than *Arabidopsis* (Ueno et al. 2015). Most of the characterized members of monocot MTPs belong to rice.

Although it is one of the most important staple crops in the world, knowledge on the metal transporters of wheat is scarce. Such information would aid in the development of wheat varieties that translocate more Fe and Zn to their seeds or that are more tolerant to metal stresses. This work aimed to identify and characterize wheat MTPs using various bioinformatics approaches.

Materials and methods

Mining of *MTP* genes in the wheat genome

Eight known rice MTP protein sequences,OsMTP1 (Q688R1.1), OsMTP2 (Q10LJ2.1), OsMTP3 (Q6Z7 K5.1), OsMTP4 (Q10PP8.1), OsMTP5 (Q5NA18.1), OsMTP6 (Q0DHJ5.2), OsMTP7 (Q9LDU0.1) and OsMTP8 (Q8H329.2) were retrieved from UniProtKB database (uniprot.org/). These reference sequences were queried against the *T. aestivum* (TGACv1) genome in Ensembl Plants portal (plants.ensembl.org/Triticum_aestivum/) with a near match search sensitivity using BLASTP and highest hit entries ($>e^{-90}$ value) for each genome component (A, B and D) was retrieved for use in further analyses. Subsequently, a Hidden Markov Model (HMM)

search was applied to retrieved MTP sequences in Pfam (pfam.xfam.org/) to verify the protein domains.

Sequence analysis of MTP genes/proteins

Physico-chemical features of MTP proteins were calculated using ProtParam tool (web.expasy.org/protparam/). Sub-cellular localizations were predicted in Plant-mPLoc server (csbio.sjtu.edu.cn/bioinf/plant-multi/). Membrane protein topologies of MTPs were predicted using TOPCONS (topcons.net/). MTP proteins were aligned by using Bioedit (Hall 2011). Conserved motifs in MTP sequences were predicted by MEME tool with such parameters; max number of motifs to find, 5; and min/max motif width, 6–50 (inclusive) (meme-suite.org/tools/meme; Bailey et al. 2009). Gene duplication events in *TaMTPs* were investigated using such criteria; (a) length of alignable sequence covers >75% of longer gene, and (b) similarity of aligned regions >75% (Gu et al. 2002; Ozyigit et al. 2016). Phylogenetic tree of MTP proteins was constructed by MEGA 6 using the Maximum likelihood (ML) method with 1000 bootstraps (Tamura et al. 2013). 1000 bp upstream flanks were retrieved using genomic coordinates of *TaMTP* genes via BioMart-EnsemblPlants (http://www.plants.ensembl.org/biomart/martview/; Kinsella et al. 2011). *Cis*-regulatory elements in upstream flanks were analyzed in PlantCARE database (http://www.bioinformatics.psb.ugent.be/webtools/plantcare/html/; Lescot et al. 2002). TaMTP coding sequences were scanned for TaMTP-targeted miRNAs in psRNATarget database (plantgrn.noble.org/psRNATarget/; Dai and Zhao 2011) with parameters: max expectation, 3 and target accessibility (UPE), 25. TaMTP proteins were modelled by using Phyre^2 server at intensive mode (sbg.bio.ic.ac.uk/phyre2/; Kelley et al. 2015) and structure validation was done by using Ramachandran plot (http://www.mordred.bioc.cam.ac.uk/~rapper/rampage.php/; Lovell et al. 2003). Predicted models were superposed using CLICK server, which calculates the root mean square deviation (RMSD) values based on α-carbon superposition (mspc.bii.a-star.edu.sg/minhn/; Nguyen et al. 2011).

Expression profiles of *TaMTP* genes

Expression profiles of *TaMTP* genes were retrieved from a specialized wheat database, WheatExp (http://www.wheat.pw.usda.gov/wheatexp/; Pearce et al. 2015). Coding sequences of *TaMTPs* were searched using nBLAST algorithm in this database, and highest hit entries (e-value 0.0) complying with genome component (A, B or D genome) of search sequences were downloaded for expression analysis. Expression values were calculated as FPKM (fragments per kilobase of exon per million fragments mapped) from RNA-seq datasets including a developmental time-course in five tissues (spike, root, leaf, grain and stem; Choulet et al. 2014), grain layer developmental time-course (10, 20 and 30 days after anthesis; Pfeifer et al. 2014), and senescing leaf time-course (heading date, 12 and 22 days after anthesis; Pearce et al. 2014).

Results and discussions

Identification of wheat MTP homologs

Wheat is a substantial global cereal grain essential to the human diet that is hexaploid with three genome components A, B and D. The ancestral genomes are thought to be derived from *T. urartu* (A-genome) and an unknown grass species associated with *Aegilops speltoides* (B-genome). Reportedly, the first hybridization resulted in tetraploid (AABB) emmer wheat (*T. dicoccoides*) whose hybridization again with *A. tauschii* (D-genome) raised the modern wheat *T. aestivum* (AABBDD) (International Wheat Genome Sequencing Consortium 2014). Currently, availability of an ordered draft genome of wheat allowed the metal tolerance protein (MTP) family genes to be mined by employing various bioinformatics tools and approaches (International Wheat Genome Sequencing Consortium 2014). Herein, using previously identified rice MTP (OsMTP1-8) sequences as a reference, MTP orthologs in the wheat genome were identified using blastp search with near match sensitivity and highest hit entries for each genome component A, B and D were retrieved for further analysis. The homology search and subsequent HMM verification resulted in a total of 20 MTP sequences, that are hereafter annotated as TaMTP1-8A, B or D based on the phylogenetic distribution with known rice MTPs (refer to phylogenetic analysis section; Table 1).

Protein family searches revealed that identified wheat MTPs belong to the cation efflux (cation diffusion facilitator, CDF) family (Table 2) whose members have been reported to transport Co^{2+}, Cd^{2+},

Table 1 List of known rice MTP sequences and their corresponding homologs in wheat genome

Rice MTP (UniProtKB ID)	Group with reference to Gustin et al. (2011)[b]	Wheat homolog[a]	Genome component	Wheat sequence (Ensembl)
OsMTP1 (Q688R1.1)**	MTP1	*TaMTP1A*	A	TRIAE_CS42_1AS_TGACv1_021178_AA0081220
		–	B	Absent
		TaMTP1D	D	TRIAE_CS42_1DS_TGACv1_080479_AA0248740
OsMTP2 (Q10LJ2.1)	MTP6	*TaMTP2A*	A	TRIAE_CS42_4AS_TGACv1_306995_AA1015980
		TaMTP2B	B	TRIAE_CS42_4BS_TGACv1_328624_AA1091200
		TaMTP2D	D	TRIAE_CS42_4DL_TGACv1_343272_AA1132570
OsMTP3 (Q6Z7K5.1)	MTP8	*TaMTP3A*	A	TRIAE_CS42_6AL_TGACv1_471959_AA1516250
		TaMTP3B	B	TRIAE_CS42_6BL_TGACv1_501730_AA1620290
		TaMTP3D	D	TRIAE_CS42_6DL_TGACv1_528040_AA1710910
OsMTP4 (Q10PP8.1)**	MTP8	*TaMTP4A*	A	TRIAE_CS42_4AS_TGACv1_306485_AA1008950
		TaMTP4B	B	TRIAE_CS42_4BL_TGACv1_320346_AA1036230
		TaMTP4D	D	TRIAE_CS42_4DL_TGACv1_342496_AA1115200
OsMTP5 (Q5NA18.1)	MTP9	*TaMTP5/6A**	A	TRIAE_CS42_3AL_TGACv1_197774_AA0667220
OsMTP6 (Q0DHJ5.2)		*TaMTP5/6B**	B	TRIAE_CS42_3B_TGACv1_223437_AA0782140
		*TaMTP5/6D**	D	TRIAE_CS42_3DL_TGACv1_249117_AA0838320
OsMTP7 (Q9LDU0.1)**	MTP9	*TaMTP7A*	A	TRIAE_CS42_3AS_TGACv1_211035_AA0683570
		TaMTP7B	B	TRIAE_CS42_3B_TGACv1_221584_AA0745100
		TaMTP7D	D	TRIAE_CS42_3DS_TGACv1_272888_AA0926160
OsMTP8 (Q8H329.2)	MTP12	*TaMTP8A*	A	TRIAE_CS42_2AS_TGACv1_114418_AA0367040
		TaMTP8B	B	TRIAE_CS42_2BS_TGACv1_147664_AA0486150
		TaMTP8D	D	TRIAE_CS42_2DS_TGACv1_177870_AA0586320

Wheat has a hexaploid chromosome structure with three genome components such as A, B and D

[a] Homologs were annotated based on phylogenetic distribution with eight known rice MTPs (refer to phylogenetic analysis section). Prefix "Ta" stands for *Triticum aestivum,* and the number (1–8) and letter (A, B and D) suffixes respectively show the MTP and sub-genome type

[b] Reference Arabidopsis groups were taken from Gustin et al. (2011)

* MTP5 and 6 homologs were indicated as *TaMTP5/6* due to their similar phylogenetic distributions

** OsMTP1, 4 and 7 have been physiologically characterized in other studies. In those studies, OsMTP4 and 7 were named as OsMTP8.1 and OsMTP9, respectively

Ni^{2+} in addition to Fe^{2+}, Mn^{2+} and Zn^{2+} (Ricachenevsky et al. 2013). In all wheat MTPs except TaMTP1 and TaMTP8, a zinc transporter dimerization domain, ZT_dimer (PF16916) was identified. This domain may indicate a dimerization region in complete zinc transporters since full-length members have been reported to form a homodimer during transport activity (Lu and Fu 2007; Lu et al. 2009; Kolaj-Robin et al. 2015). Identified *MTP* genes were distributed on A, B and D genomes of five wheat chromosomes (chr1-4 and 6) and they encoded a protein of 333–698 amino acid residues with 37.0–76.0 kDa molecular weight and 4.94–8.88 *pI* value, excluding TaMTP8B since it contains some undefined residues. Although the variation of the size of MTP proteins regarding to the number of amino acid residues was found to be quite large in wheat, this is not unusual for MTPs. For example, in *Arabidopsis*, AtMTP12 is approximately two times the size of AtMTP1; they have 798 and 398 amino acid residues, respectively. In accordance with the literature (Lu and Fu 2007), these proteins were mainly predicted to localize to the tonoplast having six putative TMDs with cytosolic N- and C-terminus. Metal specificity of *TaMTP* genes was assessed by using ortholog rice genes as a reference for different CDF groups according to Montanini et al. (2007).

Table 2 The primary sequence features of identified wheat MTP homologs

Wheat homolog	CDF type[b]	Protein family/domain[c]	Chr loc.[d]	Exons/ coding[e]	Protein length	MW (KDa)	*pI*	Sub-cellular localization	TMD number[f]
TaMTP1A	Zn	Cation_efflux	1AS	3/2	333	37.0	6.25	Vacuole	6/in → in
TaMTP1D	Zn	Cation_efflux	1DS	3/2	350	38.4	5.97	Vacuole	5/out → in
TaMTP2A	Fe/Zn	Cation_efflux, ZT_dimer	4AS	12/12	502	53.8	8.26	Vacuole	6/in → in
TaMTP2B	Fe/Zn	Cation_efflux, ZT_dimer	4BS	15/13	632	67.3	7.47	Vacuole	6/in → in
TaMTP2D	Fe/Zn	Cation_efflux, ZT_dimer	4DL	12/12	502	53.5	7.20	Vacuole	4/in → in
TaMTP3A	Mn	Cation_efflux, ZT_dimer	6AL	7/7	410	45.8	5.16	Vacuole	6/in → in
TaMTP3B	Mn	Cation_efflux, ZT_dimer	6BL	7/7	410	45.7	5.23	Vacuole	6/in → in
TaMTP3D	Mn	Cation_efflux, ZT_dimer	6DL	6/6	324	36.0	4.94	Vacuole	6/in → in
TaMTP4A	Mn	Cation_efflux, ZT_dimer	4AS	7/7	401	44.9	5.20	Vacuole	6/in → in
TaMTP4B	Mn	Cation_efflux, ZT_dimer	4BL	7/7	400	44.7	5.20	Vacuole	6/in → in
TaMTP4D	Mn	Cation_efflux, ZT_dimer	4DL	8/7	400	44.7	5.20	Vacuole	6/in → in
TaMTP5/6A	Mn	Cation_efflux, ZT_dimer	3AL	7/6	404	44.9	5.27	Vacuole	6/in → in
TaMTP5/6B	Mn	Cation_efflux, ZT_dimer	3B	6/6	404	45.0	5.33	Vacuole	6/in → in
TaMTP5/6D	Mn	Cation_efflux, ZT_dimer	3DL	6/6	404	45.0	5.29	Vacuole	6/in → in
TaMTP7A	Mn	Cation_efflux, ZT_dimer	3AS	5/5	380	43.1	6.20	P. membr./vacuole	6/in → in
TaMTP7B	Mn	Cation_efflux, ZT_dimer	3B	5/5	391	44.2	5.92	P. membr./vacuole	6/in → in
TaMTP7D	Mn	Cation_efflux, ZT_dimer	3DS	5/5	392	44.3	6.37	Vacuole	6/in → in
TaMTP8A	Zn	Cation_efflux	2AS	3/2	698	76.0	8.88	Nucleus/vacuole	12/in → in
TaMTP8B[a]	Zn	Cation_efflux	2BS	2/1	851	–	–	Nucleus/vacuole	14/in → in
		Cation_efflux	2DS	6/2	575	62.8	7.27	Nucleus/vacuole	11/out → in

[a] *pI* value and MW cannot be computed since sequence contains several consecutive undefined residues

[b] Metal specificity of wheat genes are attended by taking ortholog rice genes as reference CDF groups (Montanini et al. 2007)

[c] Cation_efflux (PF01545), ZT_dimer (PF16916)

[d] Chr location is designed with three alphanumeric characters e.g, first number shows the chromosomal location, second letter indicates the genome component since wheat has a chromosome structure with three genome components (A, B and D), and third letter represents the short (S) or long (L) arm of chromosome

[e] Exons show the number of available exons in specified transcripts while coding shows the number of coding exons

[f] TMD stands for transmembrane domain. In (cytoplasmic) or out (extracellular) from N to C-terminus

TaMTP1s and TaMTP8s belonged to Zn-CDFs; TaMTP2s to Fe/Zn-CDFs; and TaMTP3–7s to Mn-CDFs. Since most of the wheat MTPs belong to the group which shows specificity to Mn and Zn, MTPs may play major roles in the Mn and Zn homeostasis of wheat. In summary, putting aside some species-specific variations, primary sequence features of herein identified wheat MTPs mainly seemed to comply with previous reports.

Conserved motifs/residues in TaMTPs

The protein motifs are highly conserved amino acid residues which are considered to possibly have functional and/or structural roles in active proteins (Yamasaki et al. 2013). In this sense, the five most conserved motif sequences in identified TaMTP proteins were searched using MEME tool (Fig. 1). The set of 20 TaMTP sequences analyzed varied between 324 and 851 residues with an average length of 458 residues. Predicted motifs 1–4 were 50 amino acids in length while motif 5 was 41 residues. Motif 1 comprised with residues "VKLALWFYCRTFGN-NIVRAYAQDHYF DVITNVVGLVAAVLGDYFY WWIDP", motif 2 with "LDLMSGFILWFTHFSMK KPNKYK YPIGKKRMQPVGIIVFASVMACLGFQ V", motif 3 with "DTVRAYTFGTHYFVEVDIVLP EDMPLKEAHDIGESLQEKIEQLPEVERAF", motif 4 with "GAIILAVYTITNWSMTVWE NVVSLVGR

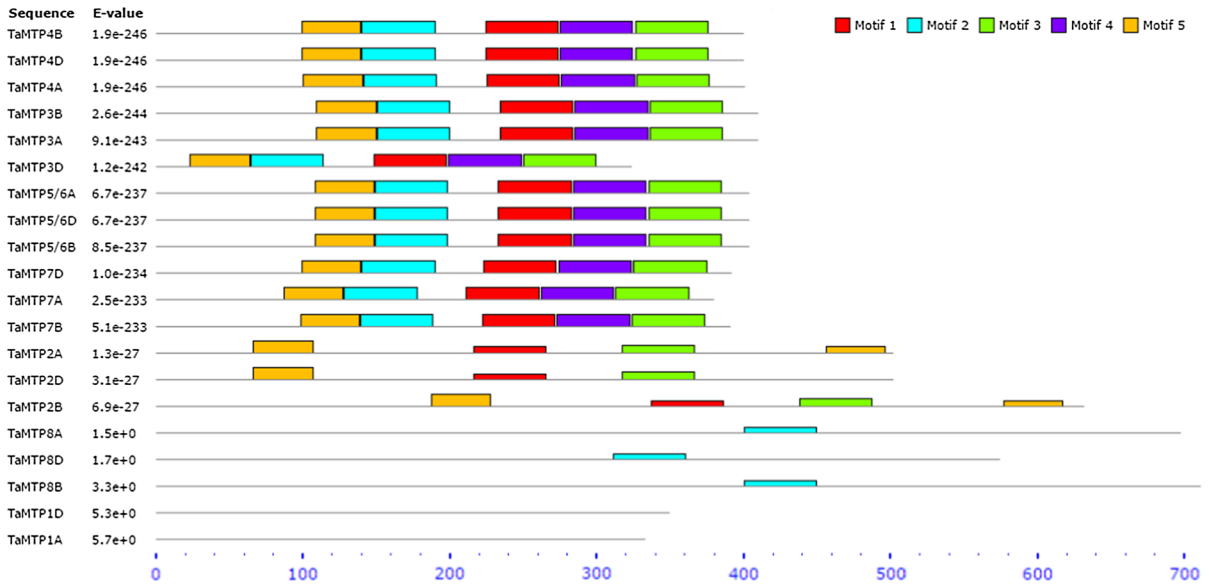

Fig. 1 The block diagram representation of five most conserved motif sequences in A, B and D genomes of 20 TaMTP proteins. Motif 2 was related with cation efflux family (Cation_efflux; PF01545), motif 3 was associated with zinc transporter dimerization domain (ZT_dimer; PF16916), and motif 1, 4 and 5 did not relate to any motifs

SAPPEYLQKLTYLCWNHDKQIRH", and motif 5 with "KQSEFAMKISN YANMVLFAGKVYA-TYRSGSMAIIASTLDSL". From these, motif 2 was related to the cation efflux family (Cation_efflux; PF01545) and motif 3 was associated with the zinc transporter dimerization domain (ZT_dimer; PF16916), while motif 1, 4 and 5 did not relate to any motifs. All TaMTP proteins, except TaMTP1, 2 and 8 members, harbored all five of these conserved motif sequences, implying that MTP variants having the same motifs may possess more similarities in their functional roles. This claim was also corroborated by analysis of the metal specificity of *TaMTP* genes, according to which TaMTP3-7 s were classified as the Mn-CDF type (also refer to Table 2). In addition, the presence of consecutive preserved motif residues in most TaMTPs, related to either the cation efflux family or zinc transporter dimerization domain, indicate that MTP structures in wheat are well conserved.

Moreover, to have further insights about this conservation, identified MTP sequences were multiple-aligned by ClustalW, and identical and similar residues respectively were shaded as black and grey (Fig. 2). The approximate location of the zinc transporter dimerization domain (ZT_dimer; PF16916) is specified with a red rectangle on the alignment in which TaMTP3-7 sequences were found to be significantly conserved. On the other hand, it was less conserved in TaMTP2 members. Sites corresponding to these residues were diverged in TaMTP1 and 8 sequences, since they do not contain zinc transporter dimerization domain. In addition, approximate locations of five identified motifs were also specified with different colored rectangles (motif 1 with orange, motif 2 with blue, motif 3 with purple, motif 4 with green and motif 5 with brown). Among these, motives 3 (completely) and 4 (partially) showed higher significance, since they are localized within the dimerization domain. The alignment also revealed that A, B and D genomes of TaMTP3-7 sequences are significantly conserved between themselves, this could be associated with their functional similarities in metal homeostasis as mentioned earlier (refer to Table 2). In contrast, TaMTP1 and 8 members demonstrated a significant divergence from others, inferring their involvement in different processes. Interestingly, Gly (G) in motif 2, and Asp (D) and His (H) in motif 1 were also found to be strictly preserved in all wheat MTP sequences, which may indicate specific functions for these amino acids.

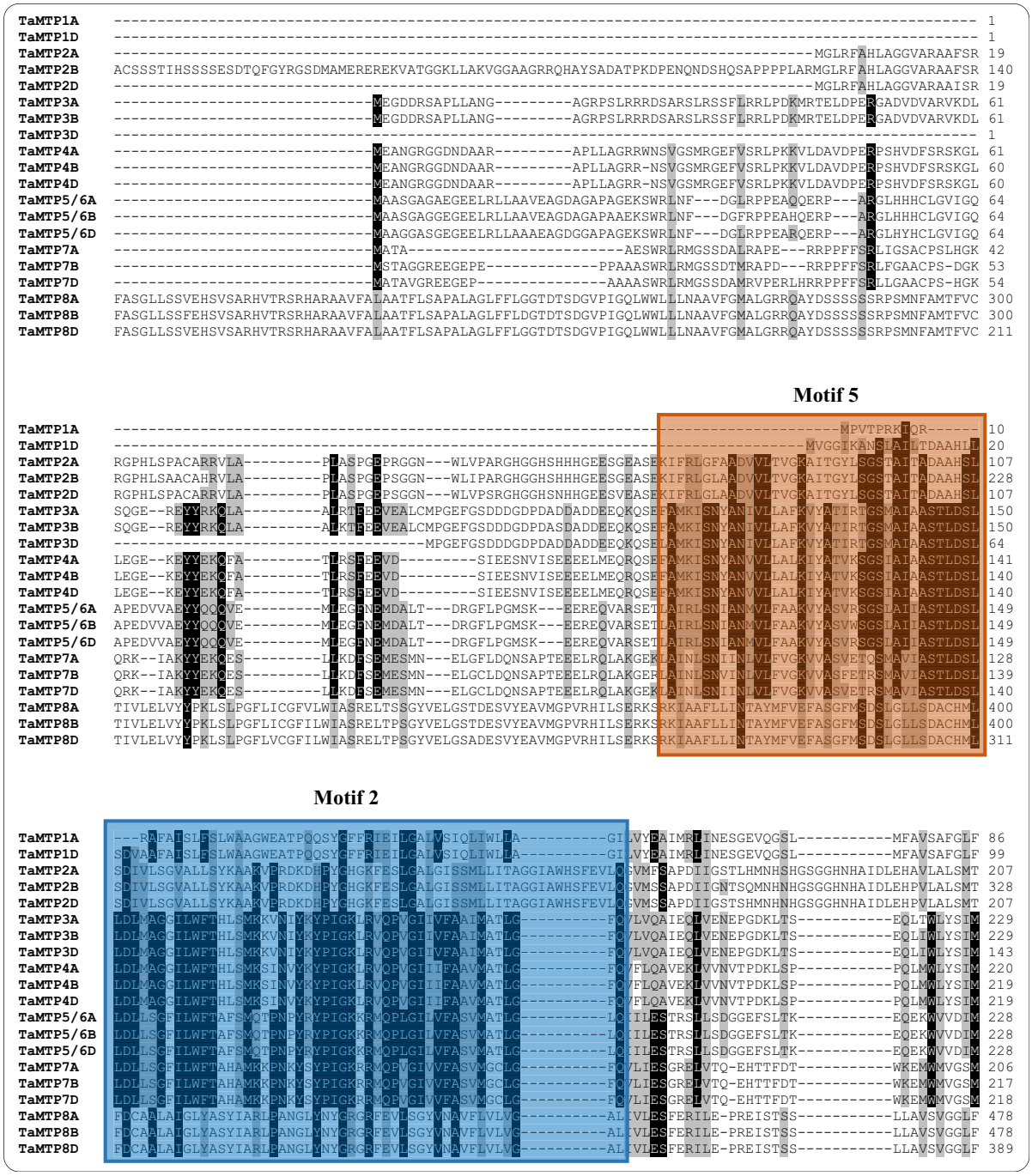

Fig. 2 Multiple sequence alignment of identified 20 wheat TaMTP (A, B and D genomes) protein sequences. The relevant identical and similar residues are shaded as *black* and *grey* respectively. *Red rectangle* approximately covers the site of zinc transporter dimerization domain (ZT_dimer; PF16916). The approximate localization of identified motifs is specified with *different color rectangles* such as motif 1 is with *orange*, motif 2 with *blue*, motif 3 with *purple*, motif 4 with *green* and motif 5 with *brown*

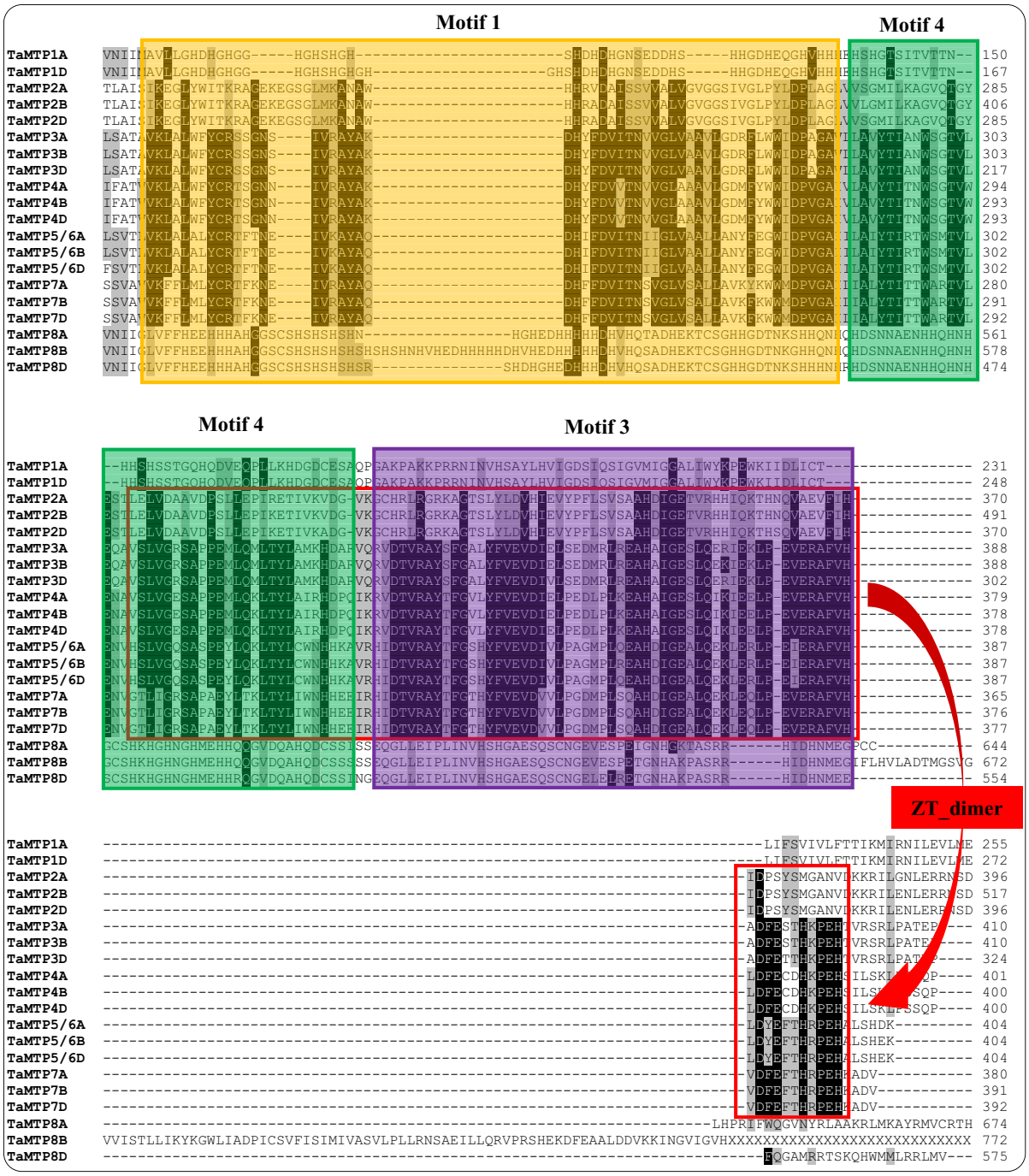

Fig. 2 continued

Chromosomal locations of TaMTPs

It has been reported that the large size and polyploid nature of the wheat genome have been major constraints in genome analyses. In addition, the hexaploid wheat genome has been highly dynamic with significant reductions in the size of gene families upon domestication and polyploidization, and with the abundance of gene fragments (Brenchley et al. 2012). To reveal further insights into functional

diversifications, possible gene duplication events in wheat TaMTP members were analyzed. 20 *TaMTP* genes were mapped on five wheat chromosomes (chr1–4 and 6; refer to Table 2). The chromosomes 1A and 1D included the *TaMTP1A* and *TaMTP1D* genes respectively; chromosomes 2A, 2B and 2D respectively had *TaMTP8A*, *TaMTP8B* and *TaMTP8D* genes; chromosomes 3A, 3B and 3D contained *TaMTP5–7A, TaMTP5–7B* and *TaMTP5–7D* genes respectively; chromosomes 4A, 4B and 4D respectively included *TaMTP2A* and *4A, TaMTP2B* and *4B,* and *TaMTP2D* and *4D* genes; and chromosome 6 had *TaMTP3A, TaMTP3B* and *TaMTP3D* genes respectively. Accordingly, A, B and D genomes of chromosomes 3 and 4 possessed a maximum of 2 *TaMTP* genes for each, while each genome component of other chromosomes contained only a single *TaMTP* gene. Genomic duplications are considered to be an essential driving force in evolution of plants. Segmental duplications refer to DNA sequences with an identity rate usually more than >90%, ranging from 1 to 400 kb in length and occur on multiple sites within the genome (Ramsey and Schemske 1998). Segmental duplications occur on different chromosomes, contrasting to tandem duplications which occur on the same chromosomes (Cannon et al. 2004). Herein, the segmental-like duplications are found within each MTP group in A, B and D genomes. This implies that MTPs from each genome donor, *T. urartu* (A-genome), *A. speltoides* (B-genome) and *A. tauschii* (D-genome) either may have been ancestrally similar to each other or originally divergent MTPs could have been stabilized during long domestication process.

Phylogenetic distribution of wheat and rice MTPs

Another main objective of this work was to comparatively investigate the phylogenetic distribution of identified wheat MTP sequences along with known rice MTPs and to infer functional relationships at the cross-species level. In this concept, phylogeny was constructed with the ML method using a total of 28 sequences from eight rice MTPs and 20 wheat homologs (Fig. 3). Based on the distribution of sequences and clustering topology, the tree was divided into seven major groups; group MTP1–4, 5/6, 7 and 8. Each rice MTP had three corresponding homologs in the wheat genome since wheat has three genome components; A, B and D. However, rice MTP1 was only present in A and D genomes but could not be identified in the B genome for the adopted search parameters. In phylogeny, group MTP1 included two TaMTPs and OsMTP1. OsMTP1 has been previously thoroughly characterized. OsMTP1 was recovered from a cDNA library screening in which Cd responsive genes were sought in rice roots (Yuan et al. 2012). Based on yeast complementation assays and elemental analysis of OsMTP1 overexpressor and knock-out mutants, OsMTP1 was proposed to transport a wide range of metals including Zn, Fe, Co, Ni, Arsenic (As)(Yuan et al. 2012; Menguer et al. 2013, Das et al. 2016). In group MTP4, three TaMTPs clustered together with OsMTP4. OsMTP4, also called OsMTP8.1, has been characterized to transport Mn rather specifically to confer Mn tolerance to rice plants by sequestrating excess Mn in the aerial parts (Chen et al. 2013). In group MTP7, three TaMTPs and an OsMTP7 were together. Contrasting to other characterized rice MTPs which localize to the tonoplast, OsMTP7 localizes to the plasma membrane and is involved in the radial transport of Mn in the roots (Ueno et al. 2015). OsMTPs in other groups have not yet been characterized. According to the phylogenetic analysis (Fig. 3), group MTP1 and 8 members were clearly diverged from other MTPs, which is in agreement with alignment and protein domain analyses (refer to Figs. 1, 2). Moreover, a further phylogeny was also constructed using wheat, rice and *Arabidopsis* MTPs altogether to figure out homologous sequences between monocots and dicots (Suppl. File). *Arabidopsis* MTPs and their putative transport element specificities were obtained from Ricachenevsky et al. (2013). In phylogeny, Mn-CDFs, Fe/Zn-CDFs and Zn-CDFs showed a clear separation where monocot OsMTP3–7 and dicot AtMTP8–11 were identified as functional Mn-CDF orthologs, OsMTP2 and AtMTP6–7 as functional Fe/Zn-CDF orthologs, and OsMTP1, 8 and AtMTP1–5, 12 as functional Zn-CDF orthologs. Phylogenetic distributions can be employed as a benchmark to infer structure and functional roles across species (Sze et al. 2014; Vatansever et al. 2016). Thus, wheat MTP sequences can be functionally inferred in relation to their respective homologs. Nevertheless, to infer more precise roles to the identified TaMTP variants, further molecular and physiological experimental characterization is required.

Promoter site and miRNA-target analysis of TaMTPs

This study also attempted to understand the regulation of the identified *TaMTP* genes at the transcriptional level. It was thus imperative to have insights about the upstream regions of genes from the transcription start-site (TSS; Ravel et al. 2015). 1000 bp upstream flanks of *TaMTP* genes were retrieved using genomic coordinates of genes via EnsemblPlants-BioMart and supplied to the PlantCARE database for *cis*-regulatory element analysis. Excluding unknown motifs, a total of 64 different cis-*elements* have been identified in upstream regions of *20 TaMTP* genes and to better characterize these large number of motifs a heatmap was constructed based on the availability of elements in each corresponding gene (Fig. 4). *Cis*-regulatory elements CAAT-box, TATA-box (except for MTP5/6A) and G-box were commonly shared by all *TaMTP* genes. Notably, CAAT- and TATA boxes are two common *cis*-regulatory elements in upstream regions of eukaryotic genes. Particularly, CAAT-box, located ∼ 80 bp upstream site, forms a binding site for RNA transcription factors and also is a key regulatory motif in modulation of the expression frequency of genes (Laloum et al. 2013). TATA-box is another core element in upstream regions of eukaryotic genes. It forms the binding site for general transcription factors or histone proteins and its binding factor may also involve in the transcription process (Bae et al. 2015). Another *cis*-element, G-box, was found in the promoter regions of all *TaMTPs*. G-box, mainly present in promoters of light-responsive genes, is reported to be involved in the light-responsive processes and its binding factors are usually demonstrated to be members of bHLH, bZIP and NAC families (Kircher et al. 1998; Toledo-Ortiz et al. 2003; Liu et al. 2016). Additionally, the promoter regions of most *TaMTP* genes also harbored *cis*-regulatory elements such as Sp1 (light responsiveness), CGTCA- and TGACG-motifs (methyl jasmonate responsiveness), ABRE (abscisic acid responsiveness), GCN4- and Skn-1 motifs (endosperm expression) and MBS (drought inducibility). Moreover, many other *cis*-regulatory elements present in promoter regions of *TaMTPs* genes were broadly categorized as common *cis*-acting elements, light responsive elements, hormone responsive elements, tissue-specific elements, and stress responsive and other elements based on their putative

Table 3 Predicted miRNAs for TaMTP transcripts, their targeting positions and inhibition type

miRNA Type	Target TaMTP	miRNA length	Target Start–end	miRNA Aligned fragment	Target Aligned fragment	Inhibition Type
ath-miR837-3p	TaMTP1A	1–20	239–258	AAACGAACAAAAAAACUGAUG	UAUCAGCUUUUGGUUUGUUU	Translation
ath-miR837-3p	TaMTP1D	1–20	278–297	AAACGAACAAAAAAACUGAUG	UAUCAGCUUUUGGUUUGUUU	Translation
mtr-miR319b-5p	TaMTP2B	1–20	1050–1069	GAGCUUUCUUUAGUCCACUC	GAGUGGGCUGAUGAAAGCUA	Translation
mtr-miR319b-5p	TaMTP2D	1–20	687–706	GAGCUUUCUUUAGUCCACUC	GAGUGGGCUGAUGAAAGCUA	Translation
stu-miR8041a-5p	TaMTP7B	1–20	161–180	GUGCUUUGCUAUUUUCAUUG	AAAGGAAAAUAGCAAAGUAC	Cleavage
stu-miR8041b-5p	TaMTP7B	1–20	161–180	GUGCUUUGCUAUUUUCAUUG	AAAGGAAAAUAGCAAAGUAC	Cleavage
osa-miR1858a	TaMTP8A	1–20	571–591	GAGAGGAGG-ACGGAGUGGGG	UCCCACUCCGUGCUUCUUCUC	Translation
osa-miR1858b	TaMTP8A	1–20	571–591	GAGAGGAGG-ACGGAGUGGGG	UCCCACUCCGUGCUUCUUCUC	Translation
mtr-miR5253	TaMTP8A	1–20	1548–1567	GAUGAAAAUGAUUAUGUUGG	CCAUCAUGAUCAUGUUCAUC	Cleavage
gma-miR5772	TaMTP8A	1–23	1496–1518	AGAAUGUGAGUUAGAGUGAGCAU	GUUCCCACUCUCACAUUCACAUUCU	Cleavage
osa-miR1858a	TaMTP8B	1–20	571–591	GAGAGGAGG-ACGGAGUGGGG	UCCCACUCCGUGCUUCUUCUC	Translation
osa-miR1858b	TaMTP8B	1–20	571–591	GAGAGGAGG-ACGGAGUGGGG	UCCCACUCCGUGCUUCUUCUC	Translation
mtr-miR5253	TaMTP8B	1–20	1599–1618	GAUGAAAAUGAUUAUGUUGG	CCAUCAUGAUCAUGUUCAUC	Cleavage
gma-miR5772	TaMTP8D	1–20	1232–1251	AGAAUGUGAGUUAGAGUGAG	CUCACUCCCAUUCACAUUCU	Cleavage

functions. Particularly, most *cis*-regulatory motifs in *TaMTP* genes were mainly associated with light responsive elements such as ACE, Box I, box II, GATA-motif, GT1-motif, I-box, LS7, TCT-motif, Box 4, CATT-motif, GA-motif, GAG-motif, L-box, MNF1, TCCC-motif, 4 cl-CMA2b, AAAC-motif, ATCT-motif, LAMP-element, rbcS-CMA7a, MRE, chs-CMA1a, 3-AF1 binding site and AE-box. Significantly, many other phytohormone-related *cis*-elements were also identified in *TaMTP* promoters including SARE and TCA-element (salicylic acid responsiveness), ERE (ethylene responsiveness), TGA-element and AuxRR (auxin responsiveness), ABRE and motif IIb (abscisic acid responsiveness), and P-box, TATC-box and GARE-motif (gibberellin responsive element). Additionally, tissue-specific *cis*-regulatory elements such as the CCGTCC-box, dOCT, NON-box and CAT-box (meristem), motif I (root), RY-element (seed), as-2-box (shoot), and HD-Zip 1 and 2 (leaf) were also found in the promotors of *TaMTP* genes. Furthermore, upstream regions of *TaMTP* genes also harbored the TC-rich repeats (defense/stress responsiveness), ARE and GC-motif (anaerobic induction), EIRE and Box-W1 (elicitor responsiveness), LTR and HSE (temperature responsiveness), C-repeat/DRE (cold and dehydration

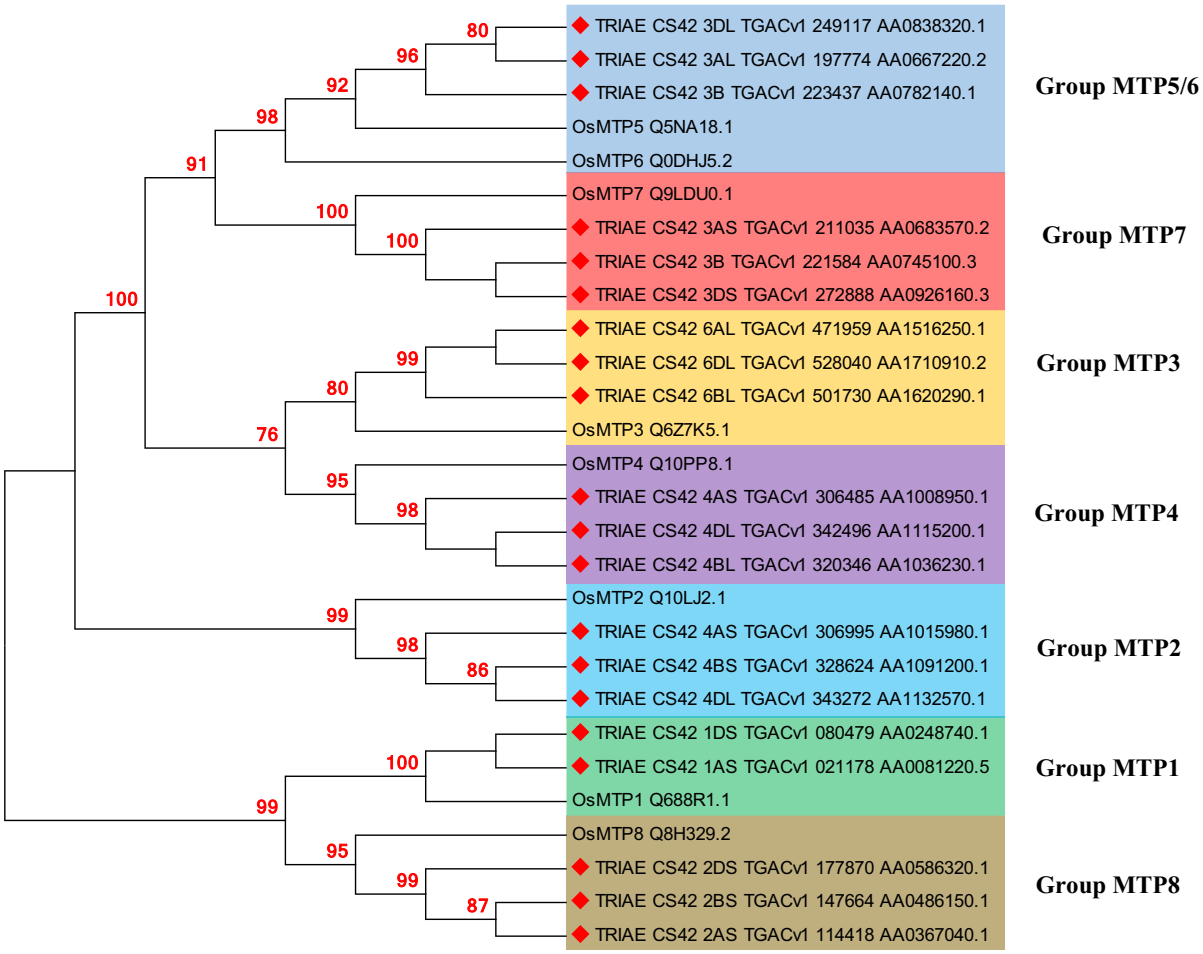

Fig. 3 Phylogenetic distribution of identified wheat and known rice MTP sequences. Phylogeny was constructed with ML method using a total of 28 sequences from eight rice MTPs (OsMTP1-8) and 20 wheat homologs (marked with *red diamonds*). Phylogeny was divided into seven major groups based on distribution of sequences such as group MTP1-4, 5/6, 7 and 8. Each rice MTP has three corresponding homologs in wheat genome since wheat has three genome components as A, B and D. However, rice MTP1 was only present in A and D genomes but could not be identified in B genome

responsiveness), circadian (circadian control), and O2-site (zein metabolism regulation) elements. Taken together, the presence of very diverse *cis*-regulatory elements associated with various metabolic processes indicates the intricate but very dynamic regulation of *TaMTP* genes.

Furthermore, potential miRNAs targeting TaMTP transcripts were also investigated to give insights into the post-transcriptional regulation of wheat genes. miRNAs are short (~21–25 nucleotides) but highly conserved non-coding RNA sequences and they perform their functions either by degrading the target mRNAs or by repressing their translations (Kumar 2014). miRNAs are accounted to regulate about 10–30% of genes in higher eukaryotes (Cui et al. 2006). They are reported to regulate various metabolic processes including development and differentiation, various biotic/abiotic stresses, signal transduction and morphogenesis (Lv et al. 2012). Herein, a scan of the 20 *TaMTP* coding sequences against all published miRNAs from different species resulted in a total of 14 potential miRNAs (Table 3). TaMTP1A and D were targeted by ath-miR837-3p with translation inhibition; TaMTP2B and D were targeted by mtr-miR319b-5p with translation inhibition; TaMTP7B was targeted by stu-miR8041a/b-5p with cleavage inhibition; TaMTP8A was targeted by gma-miR5772 and mtr-miR5253 with cleavage, and by osa-miR1858a/b with translation inhibition; TaMTP8B was targeted by mtr-miR5253 with cleavage and by osa-miR1858a/b with translation inhibition; and TaMTP8D was targeted by gma-miR5772 with cleavage inhibition. Notably, inferring from alignment and phylogenetic analyses (refer to Figs. 2, 3) the herein predicted miRNAs mainly targeted the members of most diverged groups, implying that their susceptibility for degradation may be related to their functions. In previous works, miR837-3p was reported to be involved in phosphate signal transduction in tomato leaves (Gu et al. 2010). A miR837-3p target was possibly involved in the oxidative pentose phosphate pathway (Meng et al. 2012). miR837-3p was increased in response to nitrogen and sulfur deficiencies but decreased under carbon deficiency (Liang et al. 2015). miR837-3p was significantly downregulated under Cu stress in *Paeonia ostii* seedlings (Jin et al. 2015). miR319a-5p with most other miRNAs were highly expressed under shading conditions in maize (Yuan et al. 2016). Expression of miR319a-5p was implicated in rhizomes of *Oryza longistaminata* (Zong et al. 2014) and in the flowering of *Oryza rufipogon* (Chen et al. 2013a, b). gma-miR319a-5p was reported as one of the most important restorer gene families in plants (Chen and Liu 2014). miR5772 and miR5253 were differentially expressed in tolerant and sensitive cultivars of pepper leaves under high temperatures and high air humidity (Xu et al. 2015). Osa-miR1858a/b was reported to be regulated by southern rice black-streaked dwarf virus (SRBSDV) infection in rice (Xu et al. 2014).

Fig. 4 Distributions of putative *cis*-regulatory elements in 1000 bp upstream regions of 20 *TaMTP* genes. Available motifs in corresponding genes are specified with *green boxes* otherwise with *reds* (*right side*). Motifs are also demonstrated with different colors based on their putative functions (*left side*) such as *blue* (*cis*-acting elements), *orange* (light responsive elements), *green* (hormone responsive elements), *yellow* (tissue-specific elements) and *grey* (stress responsive and other elements). Unknown function motifs are not shown herein

Temporal and spatial expression of *TaMTP*s

In order to build a basis to predict physiological functions of MTPs in wheat, organ level expression of *MTP*s in a time-course was analyzed by using publicly available transcriptome data. During a developmental time course, the expression of *MTP*s showed organ specificity (Fig. 5; Suppl. File). Interestingly, *MTP5/6*s were expressed mostly in leaves and not in roots, whereas *MTP7*s expression showed the opposite pattern. *MTP4*s were expressed in the root as well as in the shoot, unlike its closest ortholog in rice, which was solely expressed in the shoot (Chen et al. 2013). In grains, all analyzed MTPs were first sharply downregulated at 14 DAA (grain_Z71 to grain_Z75) and then upregulated at 30 DAA (grain_Z75 to grain_Z85). The only exception to that was *MTP7*s, which showed a gradual decrease in their transcript levels. Notably n leaves, all three *MTP5/6* showed a clear upregulation as the leaf aged. In root, *MTP1*s and *MTP7*s were expressed highly. In spikes the *MTP3*s, *MTP4*s and *MTP7*s were upregulated developmentally. In stems, *MTP1*s were downregulated, while *MTP3*s were upregulated gradually during development. As the second node of wheat formed (z32), expression of *MTP7*s peaked. Overall, the temporal and spatial regulation of *MTP*s may indicate that MTPs are actively involved in maintaining wheat nutrient homeostasis throughout its life cycle.

Motifs	Putative Function	MTP1A	MTP1D	MTP2A	MTP2B	MTP2D	MTP3A	MTP3B	MTP3D	MTP4A	MTP4B	MTP4D	MTP5/6A	MTP5/6B	MTP5/6D	MTP7A	MTP7B	MTP7D	MTP8A	MTP8B	MTP8D
CAAT-box	common *cis*-acting element																				
TATA-box	core promoter element																				
5UTR Py-rich stretch	conferring high transcription levels																				
ACE	light responsiveness																				
Box I	light responsiveness																				
box II	light responsiveness																				
G-Box	light responsiveness																				
GATA-motif	light responsiveness																				
GT1-motif	light responsiveness																				
I-box	light responsiveness																				
LS7	light responsiveness																				
Sp1	light responsiveness																				
TCT-motif	light responsiveness																				
Box 4	light responsiveness																				
CATT-motif	light responsiveness																				
GA-motif	light responsiveness																				
GAG-motif	light responsiveness																				
L-box	light responsiveness																				
MNF1	light responsiveness																				
TCCC-motif	light responsiveness																				
4cl-CMA2b	light responsiveness																				
AAAC-motif	light responsiveness																				
ATCT-motif	light responsiveness																				
LAMP-element	light responsiveness																				
rbcS-CMA7a	light responsiveness																				
MRE	light responsiveness																				
chs-CMA1a	light responsiveness																				
3-AF1 binding site	light responsiveness																				
AE-box	light responsiveness																				
CGTCA-motif	MeJA responsiveness																				
TGACG-motif	MeJA responsiveness																				
SARE	salicylic acid responsiveness																				
TCA-element	salicylic acid responsiveness																				
ERE	ethylene responsiveness																				
TGA-element	auxin responsiveness																				
AuxRR-core	auxin responsiveness																				
ABRE	abscisic acid responsiveness																				
motif IIb	abscisic acid responsiveness																				
P-box	gibberellin responsive element																				
TATC-box	gibberellin responsiveness																				
GARE-motif	gibberellin responsive element																				

Senescence is associated with an extensive micronutrient remobilization from leaves to seeds. In accordance with that, in wheat, the disruption of *Gpc-B1*, a gene encoding a NAC transcription factor involved in the regulation of leaf senescence, resulted in seeds with low concentrations of Fe

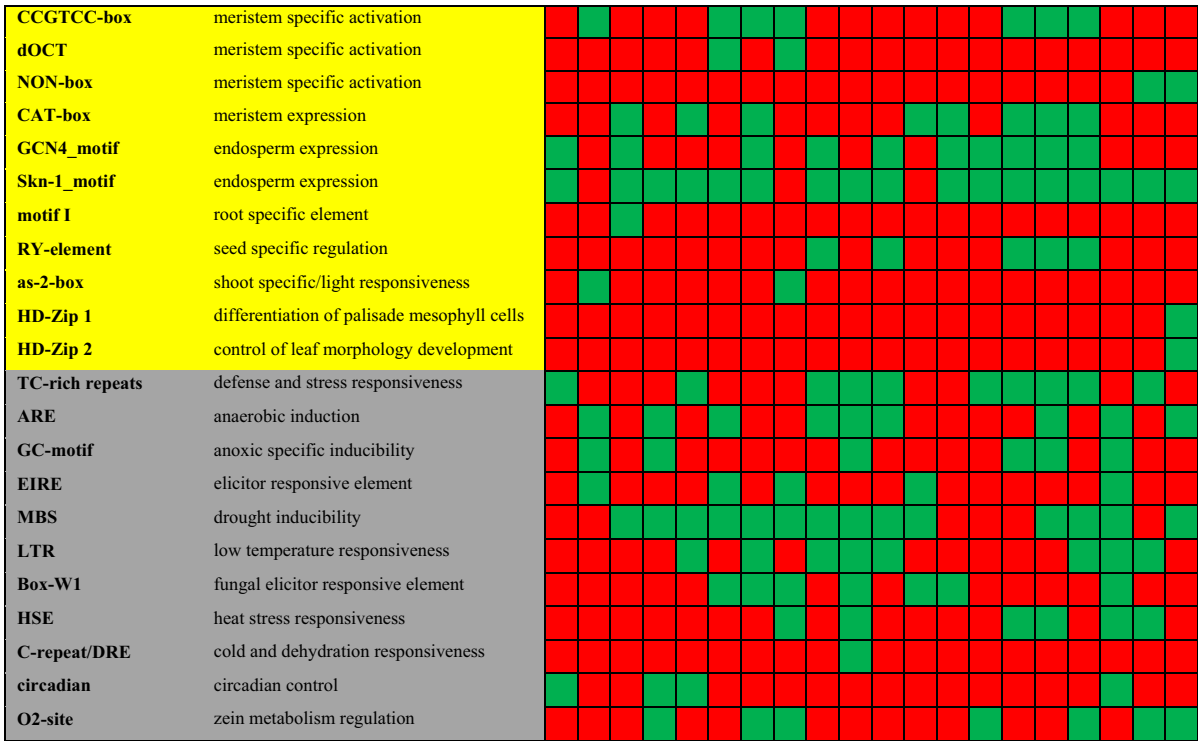

Fig. 4 continued

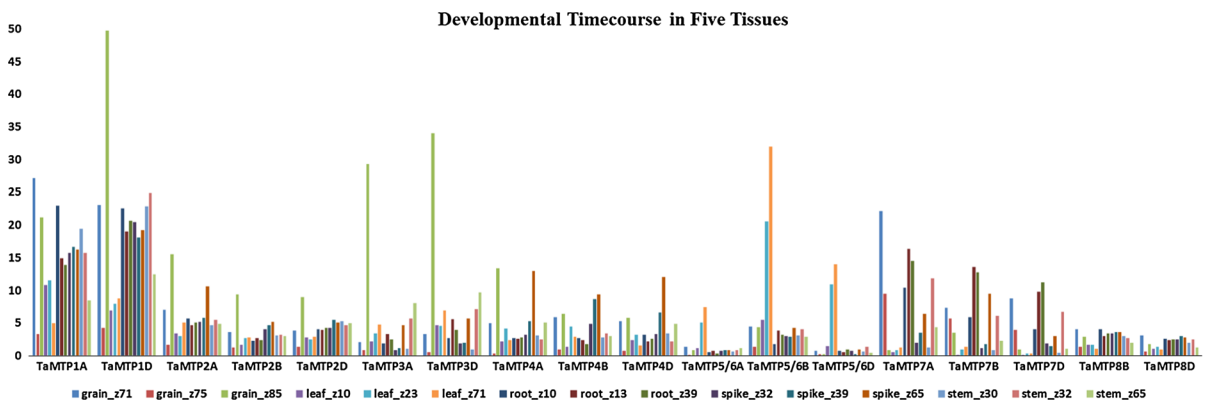

Fig. 5 Expression profiles of *TaMTP* genes during developmental timecourse of grain, leaf, root, spike and stem. Expression values are specified as FPKM (Fragments Per Kilobase Of Exon Per Million Fragments Mapped). Developmental timecourses are based on Zadoks cereal developmental scale (refer to Suppl. File)

and Zn (Uauy et al. 2006). This was accompanied by higher concentrations of these elements in the flag leaf, underlining the source-sink relationship between the flag leaf and seed during senescence. In order to investigate MTPs involvement in metal homeostasis in senescencing wheat, *MTP* activity in both flag leaf and seed was analyzed. Expression analysis of *MTP*s in the flag leaf revealed that, with an exception of a slight downregulation of Ta*MTP5/6B*, none of the *MTP*s transcriptionally responded to senescence (Fig. 6; Suppl. File). This data indicated that MTPs are not primarily involved in the remobilization of micronutrients from senescencing leaves.

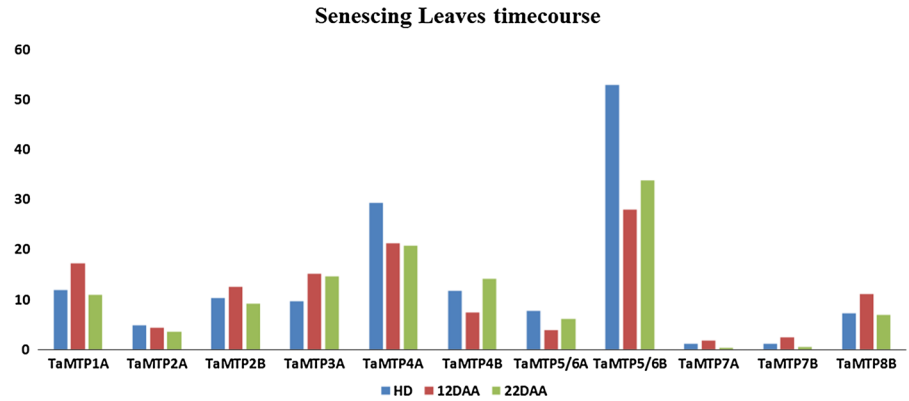

Fig. 6 Expression profiles of *TaMTP* genes in senescing leaves timecourse. Expression values are specified as FPKM. HD, heading date and DAA, days after anthesis

In seeds of wheat, metal micronutrients are not homogeniously distributed, but instead show organ and tissue level specificity. Most of the Fe, Mn and Zn are found in the aleurone layer of seeds and the embryo; while the endosperm,the largest part of the seed, is poor of these micronutrients (Mazzolini et al. 1985; Borg et al. 2009; Regvar et al. 2011). In order to investigate the possible involvement of MTPs in storage mineral accumulation, activity of *MTPs* in wheat seeds was analyzed (Fig. 7; Suppl. File). Surprisingly, in general *MTP* transcript levels were found to be high and regulated throughout development. *TaMTP*s that were expressed highly in the endosperm included *TaMTP1*s, *TaMTP2*s, and *TaMTP7A*. Expression of *TaMTP5/6*s in the seeds was high but confined to the aleurone layer. Interestingly, all MTPs were preferentially expressed in the aleurone during grain filling (20DPA and 30DPA). The aleurone layer of the grain stores minerals, subcellularly in the globoids of the vacuoles (Regvar et al. 2011). Sequestration of storage minerals into vacuoles requires tonoplast localized transporter proteins as shown in *Arabidopsis* for Fe (Kim et al. 2006) and for Mn (Eroglu 2015). Thus, considering that they are usually localized to tonoplasts (Fig. 2), TaMTPs are likely to be involved in making up mineral reserves in the vacuoles of cells in the aleurone layer of wheat grains. In particular, since the closest orthologs of TaMTP1s were characterized as a tonoplast-bound Zn transporter in both *Arabidopsis* and rice, TaMTP1s may be responsible for higher Zn contents in the vacuoles of the aleurone tissue. In summary, temporal and spatial expression of *TaMTP*s indicated that they are not likely to play major roles in metal remobilization in senescencing leaves, but instead are likely to be involved in reserve metal accumulation by providing an intercellular sink by effluxing metals out of the cytosol.

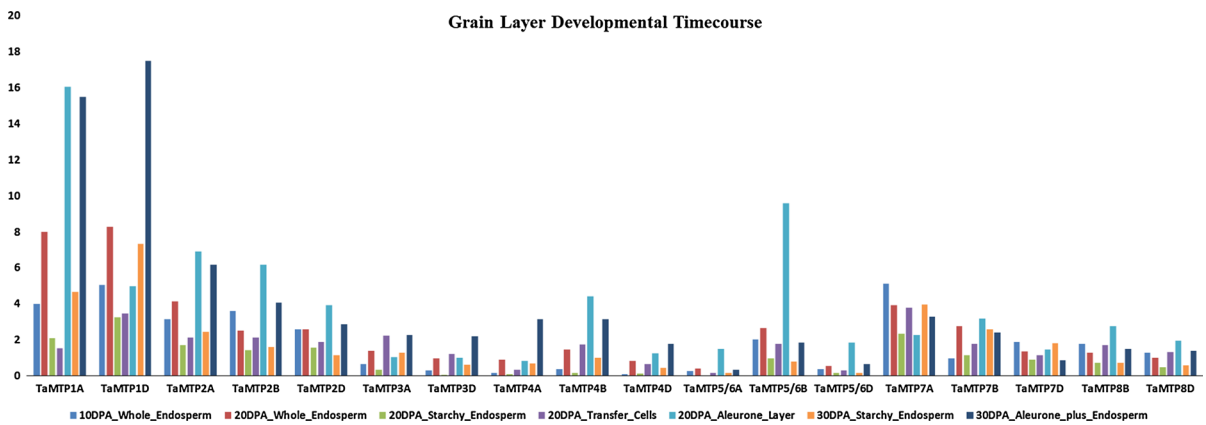

Fig. 7 Expression profiles of *TaMTP* genes in grain layer developmental timecourse. For localization of grain layers refer to supplementary file. Expression values are specified as FPKM. DPA, days after anthesis

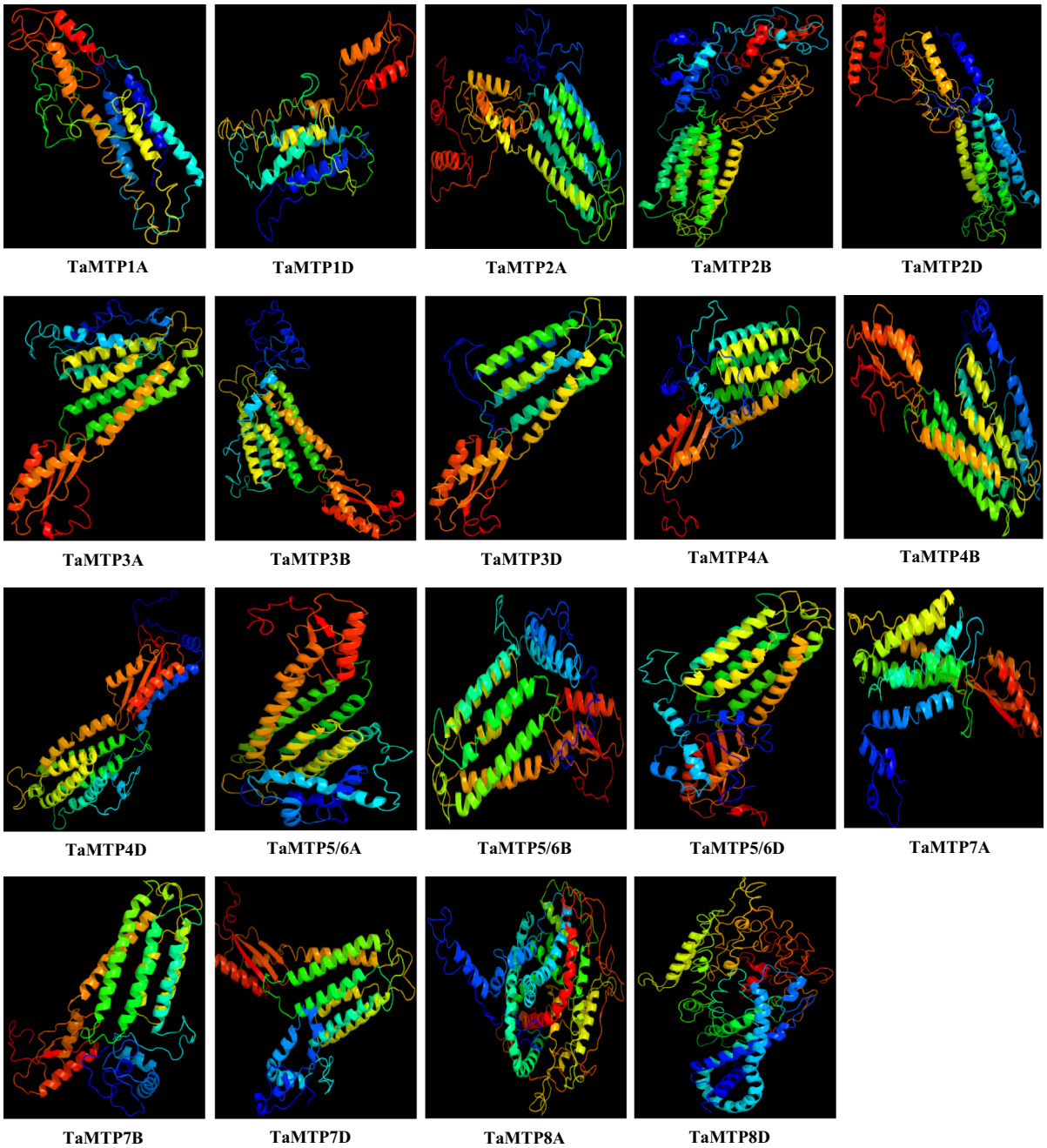

Fig. 8 Predicted 3D models of wheat TaMTP proteins. Models were generated by using Phyre[2] server at intensive mode. TaMTP8B structure could not be satisfactorily predicted since it contained some consecutive undefined residues. Models were visualized by rainbow color from N to C terminus and organized in order as TaMTP1-8A, B and D

Homology modelling of TaMTP proteins

Finally, all 20 wheat TaMTP members, except for TaMTP8B which contained several consecutive undefined residues in its protein sequence, were modelled using Phyre[2] server at intensive mode (Fig. 8). Predicted models were based on following templates to heuristically maximize the alignment

coverage, percentage identity and confidence score for the tested sequences. Two templates, 2QFI and 3J1Z from structures of zinc transporter YiiPs were used in the modelling of TaMTP1A/D, TaMTP3A/B/D, TaMTP4A, TaMTP5/6A/B/D and TaMTP8A; templates 5ENS (from bacterial efflux pump), 2QFI and 3J1Z in TaMTP2A/D models; templates 2QFI, 3J1Z, 1GHH (from *E. coli* DinI protein) and 1IWG (from bacterial multidrug efflux transporter AcrB) in TaMTP2B model; templates 2ENK (from human solute carrier family 30/Zn transporter), 2QFI and 3J1Z in TaMTP4B/D and TaMTP7A models; templates 2ENK, 5A39 (from Rad14), 1D4U (from human nucleotide excision repair protein XPA), 2QFI and 3J1Z in TaMTP7B model; templates 2QFI, 3J1Z and 4L6R (from human glucagon G protein coupled receptor) in TaMTP7D model; and templates 2QFI, 3J1Z, and 5GAS (from *Thermus thermophilus* V/A-ATPase) employed in TaMTP8D model. The quality of models was validated by Ramachandran plot analysis in which >80% of residues were in allowed region indicating the fairly good structures of models. However, it was apparent that to construct more reliable, native-like models the more experimentally solved structures are required from CDF family proteins in particular from plant MTPs. The α-helices primarily constituted the secondary structures of modelled wheat proteins with 48–67% whereas β-strands distributed with a 1−10%.Ttransmembrane (TM) helices possessed a percentage of 19-38 in secondary structure of TaMTPs with mainly six putative TMDs. Moreover, to figure out the similarity or divergence of generated models, structures were superimposed to calculate the percentages of structure overlap. The structure overlap is regarded as e.g, given X and Y proteins the percentage of representative atoms in X protein that is within 3.5 Å of the respective atoms in the superimposed Y protein. The calculations were emphasized on the A, B and D genomes of each TaMTP group within itself (refer to phylogenetic section) to estimate how preserved each genome component during long hybridization and polyploidization processes were structurally, and thereby also functionally. The superimposed TaMTP1A-D models were indicated by 76.88% structure overlap, TaMTP2A-B by 69.12%, TaMTP2A-D by 69.12%, TaMTP2B-D by 44.62%, TaMTP3A-B by 69.51%, TaMTP3A-D by 73.46%, TaMTP3B-D by 80.56%, TaMTP4A-B by 73.75%, TaMTP4A-D by 66.25%, TaMTP4B-D by 68.25%, TaMTP5/6A-B by 73.51%, TaMTP5/6A-D by 72.03%, TaMTP5/6B-D by 77.23%, TaMTP7A-B by 46.58%, TaMTP7A-D by 48.68%, TaMTP7B-D by 60.10%, and TaMTP8A-D by 33.04%. A, B and D genomes of each TaMTP group mainly demonstrated a 66-76% structural overlap. However, some models such as TaMTP2B-D (44.62%), TaMTP7A-B (46.58%), TaMTP7A-D (48.68%) and TaMTP8A-D (33.04%) showed low structure similarity but above the twilight zone (<30%). Taken together, it has been implicated that MTPs from each genome donor, *T. urartu* (A-genome), *A. speltoides* (B-genome) and *A. tauschii* (D-genome) either may have been ancestrally similar to each other or originally divergent MTPs could have been stabilized during long domestication process resulting in changes on protein structures thereby on protein functions.

Conclusion

Wheat is a globally produced cereal grain and plays a crucial role in global food security. However, potential genetic biofortification tools for wheat including the knowledge of MTPs are largely missing due to its large hexaploid genome size. This study identified 20 MTPs in wheat and annotated as TaMTP1-8A, B or D based on their phylogeny. Their preferential expression in the aleurone of the grains, indicated that *TaMTPs* contribute to build up the rich metal reserves found in this tissue. This study showed potential importance of MTPs in the biofortification of grains with essential micronutrients and will serve as a basis for the physiological characterization of wheat MTPs.

Acknowledgements We thank Benjamin Gruber for the fruitful discussion and proofreading of the article. Seckin Eroglu thanks Scientific and Technological Council of Turkey (Ankara, Turkey) for the fellowship through BIDEB-2232 program.

References

Arrivault S, Senger T, Krämer U (2006) The Arabidopsis metal tolerance protein AtMTP3 maintains metal homeostasis by mediating Zn exclusion from the shoot under Fe deficiency and Zn oversupply. Plant J 46(5):861–879

Bae SH, Han HW, Moon J (2015) Functional analysis of the molecular interactions of TATA box-containing genes and essential genes. PLoS ONE 10(3):e0120848

Borg S, Brinch-Pedersen H, Tauris B, Holm PB (2009) Iron transport, deposition and bioavailability in the wheat and barley grain. Plant Soil 325(1–2):15–24

Brenchley R, Spannagl M, Pfeifer M, Barker GL, D'Amore R, Allen AM, Kay S (2012) Analysis of the bread wheat genome using whole-genome shotgun sequencing. Nature 491(7426):705–710

Bailey TL, Boden M, Buske, FA, Frith M, Grant, CE, Clementi L & Noble WS (2009) MEME SUITE: tools for motif discovery and searching. Nucleic Acids Res, gkp335

Cannon SB, Mitra A, Baumgarten A, Young ND, May G (2004) The roles of segmental and tandem gene duplication in the evolution of large gene families in Arabidopsis thaliana. BMC Plant Biol 4(1):1

Chen L, Liu YG (2014) Male sterility and fertility restoration in crops. Annu Rev Plant Biol 65:579–606

Chen Z, Li F, Yang S, Dong Y, Yuan Q, Wang F, Pei X (2013a) Identification and functional analysis of flowering related microRNAs in common wild rice (Oryza rufipogon Griff.). PLoS ONE 8(12):e82844

Chen Z et al (2013b) Mn tolerance in rice is mediated by MTP8. 1, a member of the cation diffusion facilitator family. J Exp Bot 64(14):4375–4387

Choulet F, Alberti A, Theil S, Glover N, Barbe V, Daron J, Leroy P (2014) Structural and functional partitioning of bread wheat chromosome 3B. Science 345(6194):1249721

Clemens S, Palmgren MG, Krämer U (2002) A long way ahead: understanding and engineering plant metal accumulation. Trends Plant Sci 7(7):309–315

Cubillas C, Vinuesa P, Tabche ML, García-de los Santos A (2013) Phylogenomic analysis of cation diffusion facilitator proteins uncovers Ni^{2+}/Co^{2+} transporters. Metallomics 5(12):1634–1643

Cui Q, Yu Z, Purisima EO, Wang E (2006) Principles of microRNA regulation of a human cellular signaling network. Mol Syst Biol 2(1):46

Dai X, Zhao PX (2011) psRNATarget: a plant small RNA target analysis server. Nucleic Acids Res 39(suppl 2):W155–W159

Das N et al (2016) Enhanced cadmium accumulation and tolerance in transgenic tobacco overexpressing rice metal tolerance protein gene OsMTP1 is promising for phytoremediation. Plant Physiol Biochem 105:297–309

Delhaize E, Gruber BD, Pittman JK, White RG, Leung H, Miao Y, Richardson AE (2007) A role for the AtMTP11 gene of Arabidopsis in manganese transport and tolerance. Plant J 51(2):198–210

Eroglu S (2015) Characterization of MTP8 as a tonoplast Fe/Mn transporter essential for Fe efficiency and for Fe and Mn localization in the subepidermis of Arabidopsis embryos (Doctoral dissertation, Halle (Saale), Universitäts-und Landesbibliothek Sachsen-Anhalt, Diss., 2015)

Eroglu S, Meier B, von Wirén N, Peiter E (2016) The vacuolar manganese transporter MTP8 determines tolerance to iron deficiency-induced chlorosis in Arabidopsis. Plant Physiol 170(2):1030–1045

Fujiwara T, Kawachi M, Sato Y, Mori H, Kutsuna N, Hasezawa S, Maeshima M (2015) A high molecular mass zinc transporter MTP12 forms a functional heteromeric complex with MTP5 in the Golgi in Arabidopsis thaliana. FEBS J 282(10):1965–1979

Gu Z, Cavalcanti A, Chen FC, Bouman P, Li WH (2002) Extent of gene duplication in the genomes of Drosophila, nematode, and yeast. Mol Biol Evol 19(3):256–262

Gu M, Xu K, Chen A, Zhu Y, Tang G, Xu G (2010) Expression analysis suggests potential roles of microRNAs for phosphate and arbuscular mycorrhizal signaling in Solanum lycopersicum. Physiol Plant 138(2):226–237

Gustin JL, Zanis MJ, Salt DE (2011) Structure and evolution of the plant cation diffusion facilitator family of ion transporters. BMC Evol Biol 11(1):1

Hall T (2011) BioEdit: an important software for molecular biology. GERF Bull Biosci 2(1):6

International Wheat Genome Sequencing Consortium (2014) A chromosome-based draft sequence of the hexaploid bread wheat (*Triticum aestivum*) genome. Science 345(6194): 1251788

Jin Q, Xue Z, Dong C, Wang Y, Chu L, Xu Y (2015) Identification and characterization of microRNAs from tree peony (*Paeonia ostii*) and their response to copper stress. PLoS ONE 10(2):e0117584

Kelley LA, Mezulis S, Yates CM, Wass MN, Sternberg MJ (2015) The Phyre2 web portal for protein modeling, prediction and analysis. Nat Protoc 10(6):845–858

Kim SA, Punshon T, Lanzirotti A, Li L, Alonso JM, Ecker JR, Kaplan J, Guerinot ML (2006) Localization of iron in Arabidopsis seed requires the vacuolar membrane transporter VIT1. Science 314(5803):1295–1298

Kinsella RJ, Kähäri A, Haider S, Zamora J, Proctor G, Spudich G & Kersey P (2011) Ensembl BioMarts: a hub for data retrieval across taxonomic space. Database, bar030

Kircher S, Ledger S, Hayashi H, Weisshaar B, Schäfer E, Frohnmeyer H (1998) CPRF4a, a novel plant bZIP protein of the CPRF family: comparative analyses of light-dependent expression, post-transcriptional regulation, nuclear import and heterodimerisation. Mol Gen Genet MGG 257(6):595–605

Kobae Y, Uemura T, Sato MH, Ohnishi M, Mimura T, Nakagawa T, Maeshima M (2004) Zinc transporter of *Arabidopsis thaliana* AtMTP1 is localized to vacuolar membranes and implicated in zinc homeostasis. Plant Cell Physiol 45(12):1749–1758

Kolaj-Robin O, Russell D, Hayes KA, Pembroke JT, Soulimane T (2015) Cation diffusion facilitator family: structure and function. FEBS Lett 589(12):1283–1295

Kumar R (2014) Role of microRNAs in biotic and abiotic stress responses in crop plants. Appl Biochem Biotechnol 174(1):93–115

Laloum T, De Mita S, Gamas P, Baudin M, Niebel A (2013) CCAAT-box binding transcription factors in plants: y so many? Trends Plant Sci 18(3):157–166

Lescot M, Déhais P, Thijs G, Marchal K, Moreau Y, Van de Peer Y, Rombauts S (2002) PlantCARE, a database of plant cis-acting regulatory elements and a portal to tools for in silico analysis of promoter sequences. Nucleic Acids Res 30(1):325–327

Liang G Ai Q, Yu D (2015) Uncovering miRNAs involved in crosstalk between nutrient deficiencies in Arabidopsis. Sci Rep, 5

Liu L, Xu W, Hu X, Liu H, Lin, Y (2016) W-box and G-box elements play important roles in early senescence of rice flag leaf. Sci Rep, 6

Lovell SC, Davis IW, Arendall WB, de Bakker PI, Word JM, Prisant MG, Richardson DC (2003) Structure validation by Cα geometry: ϕ, ψ and Cβ deviation. Proteins Struct Funct Bioinformat 50(3):437–450

Lu M, Fu D (2007) Structure of the zinc transporter YiiP. Science 317(5845):1746–1748

Lu M, Chai J, Fu D (2009) Structural basis for autoregulation of the zinc transporter YiiP. Nat Struct Mol Biol 16(10): 1063–1067

Lv S, Nie X, Wang L, Du X, Biradar SS, Jia X, Weining S (2012) Identification and characterization of microRNAs from barley (Hordeum vulgare L.) by high-throughput sequencing. Int J Mol Sci 13(3):2973–2984

Marcelis LFM (1996) Sink strength as a determinant of dry matter partitioning in the whole plant. J Exp Bot 47:1281–1291

Marschner H (2012) Marschner's mineral nutrition of higher plants, vol 89. Academic press, London

Mazzolini AP, Pallaghy CK, Legge GJF (1985) Quantitative microanalysis of Mn, Zn and other elements in mature wheat seed. New Phytol 100(4):483–509

Meng Y, Shao C, Ma X, Wang H, Chen M (2012) Expression-based functional investigation of the organ-specific microRNAs in Arabidopsis. PLoS ONE 7(11):e50870

Menguer PK, Farthing E, Peaston KA, Ricachenevsky FK, Fett JP, Williams LE (2013). Functional analysis of the rice vacuolar zinc transporter OsMTP1. J Exp Bot 64(10):2871–2883

Montanini B, Blaudez D, Jeandroz S, Sanders D, Chalot M (2007) Phylogenetic and functional analysis of the Cation Diffusion Facilitator (CDF) family: improved signature and prediction of substrate specificity. BMC Genom 8(1):1

Nguyen MN, Tan KP, Madhusudhan MS (2011) CLICK—topology-independent comparison of biomolecular 3D structures. Nucleic Acids Res 39(suppl 2):W24–W28

Ozyigit II, Filiz E, Vatansever R, Kurtoglu KY, Koc I, Öztürk MX, Anjum NA (2016) Identification and comparative analysis of H2O2-scavenging enzymes (ascorbate peroxidase and glutathione peroxidase) in selected plants employing bioinformatics approaches. Front Plant Sci 7:301

Pearce S, Tabbita F, Cantu D, Buffalo V, Avni R, Vazquez-Gross H, Dubcovksy J (2014) Regulation of Zn and Fe transporters by the GPC1 gene during early wheat monocarpic senescence. BMC Plant Biol 14(1):1

Pearce S et al (2015) WheatExp: an RNA-seq expression database for polyploid wheat. BMC Plant Biol 15(1):1

Peiter E, Montanini B, Gobert A, Pedas P, Husted S, Maathuis FJ, Sanders D (2007) A secretory pathway-localized cation diffusion facilitator confers plant manganese tolerance. Proc Natl Acad Sci USA 104(20):8532–8537

Pfeifer M, Kugler KG, Sandve SR, Zhan B, Rudi H, Hvidsten TR, International Wheat Genome Sequencing Consortium (2014) Genome interplay in the grain transcriptome of hexaploid bread wheat. Science 345(6194):1250091

Qu LQ, Yoshihara T, Ooyama A, Goto F, Takaiwa F (2005) Iron accumulation does not parallel the high expression level of ferritin in transgenic rice seeds. Planta 222(2):225–233

Ramsey J, Schemske DW (1998) Pathways, mechanisms, and rates of polyploid formation in flowering plants. Annu Rev Ecol Syst 29:467–501

Ravel C, Fiquet S, Boudet J, Dardevet M, Vincent J, Merlino M, Martre P (2015) Conserved cis-regulatory modules in promoters of genes encoding wheat high-molecular-weight glutenin subunits. Adv Seed Biol, 150

Regvar M, Eichert D, Kaulich B, Gianoncelli A, Pongrac P, Vogel-Mikuš K, Kreft I (2011) New insights into globoids of protein storage vacuoles in wheat aleurone using synchrotron soft X-ray microscopy. J Exp Bot 62:3929–3939

Ricachenevsky FK, Menguer PK, Sperotto RA, Williams LE, Fett JP (2013) Roles of plant metal tolerance proteins (MTP) in metal storage and potential use in biofortification strategies. Front Plant Sci 4:144

Sze H, Chen LQ, Jez JM (2014) Evolutionary relationships and functional diversity of plant sulfate transporters. Evol Transp Plants, 63

Tamura K, Stecher G, Peterson D, Filipski A, Kumar S (2013) MEGA6: molecular evolutionary genetics analysis version 6.0. Mol Biol Evol 30(12):2725–2729

Thomine S, Vert G (2013) Iron transport in plants: better be safe than sorry. Curr Opin Plant Biol 16(3):322–327

Toledo-Ortiz G, Huq E, Quail PH (2003) The Arabidopsis basic/helix-loop-helix transcription factor family. Plant Cell 15(8):1749–1770

Uauy C, Distelfeld A, Fahima T, Blechl A, Dubcovsky J (2006) A NAC gene regulating senescence improves grain protein, zinc, and iron content in wheat. Science 314(5803): 1298–1301

Ueno D, Sasaki A, Yamaji N, Miyaji T, Fujii Y, Takemoto Y, Ma JF (2015) A polarly localized transporter for efficient manganese uptake in rice. Nature plants 1:15170

Vatansever R, Koc I, Ozyigit II, Sen U, Uras ME, Anjum NA, Filiz E (2016) Genome-wide identification and expression analysis of sulfate transporter (SULTR) genes in potato (*Solanum tuberosum* L.). Planta 244(6):1167–1183

White PJ, Broadley MR (2009) Biofortification of crops with seven mineral elements often lacking in human diets–iron, zinc, copper, calcium, magnesium, selenium and iodine. New Phytol 182(1):49–84

Xu D, Mou G, Wang K, Zhou G (2014) MicroRNAs responding to southern rice black- streaked dwarf virus infection and their target genes associated with symptom development in rice. Virus Res 190:60–68

Xu XW, Li T, Li Y, Li ZX (2015) Identification and analysis of *C. annuum* microRNAs by high-throughput sequencing and their association with high temperature and high air humidity stress. Int J Bioautom 19:459–472

Yamasaki K, Kigawa T, Seki M, Shinozaki K, Yokoyama S (2013) DNA-binding domains of plant-specific transcription factors: structure, function, and evolution. Trends Plant Sci 18(5):267–276

Yuan L, Yang S, Liu B, Zhang M, Wu K (2012) Molecular characterization of a rice metal tolerance protein, OsMTP1. Plant Cell Rep 31(1):67–79

Yuan L, Tang J, Liu J, Song H, Zhang M, Li H, Li C (2016) Differential miRNA expression in maize ear subjected to shading tolerance. Acta Physiol Plant 38(3):1–12

Zhang Y, Xu YH, Yi HY, Gong JM (2012) Vacuolar membrane transporters OsVIT1 and OsVIT2 modulate iron translocation between flag leaves and seeds in rice. Plant J 72(3):400–410

Zong Y, Huang L, Zhang T, Qin Q, Wang W, Zhao X, Li Z (2014) Differential microRNA expression between shoots and rhizomes in Oryza longistaminata using high-throughput RNA sequencing. The Crop Journal 2(2):102–109